Pergamon

Geochimica et Cosmochimica Acta, Vol. 67, No. 21, pp. 4091–4099, 2003

0016-7037/03 $30.00 + .00

doi:10.1016/S0016-7037(00)00384-3

Barium and strontium uptake into larval protoconchs and statoliths of the marine neogastropod *Kelletia kelletii*

DANIELLE C. ZACHERL,[1,3,*] GEORGES PARADIS,[2] and DAVID W. LEA[2]

[1]Department of Ecology, Evolution and Marine Biology, University of California, Santa Barbara, CA 93106, USA
[2]Department of Geological Sciences and Marine Science Institute, University of California, Santa Barbara, CA 93106, USA
[3]Department of Organismic Biology, Ecology and Evolution, University of California, 621 Charles E. Young Drive South, Los Angeles, CA 90095-1606, USA

(*Received December* 20, 2002; *accepted in revised form May* 21, 2003)

Abstract—The trace elemental composition of calcified larval hard parts may serve as useful tags of natal origin for invertebrate population studies. We examine whether the trace metal barium (Ba) deposits into the calcium carbonate matrix of molluscan larval statolith and protoconch in proportion to seawater Ba concentration at two temperatures (11.5 and 17°C). We also examine strontium (Sr) uptake as a function of temperature. Using encapsulated larvae of the marine gastropod, *Kelletia kelletii*, reared in the laboratory under controlled conditions, we demonstrate a significant inverse effect of temperature and a positive effect of seawater Ba/Ca ratio on Ba incorporation into larval carbonates. Ba/Ca partition coefficients (D_{Ba}) in protoconch were 1.13 at 11.4°C and 0.88 at 17.1°C, while D_{Ba} in larval statolith measured 1.58 at 11.4°C and 1.29 at 17.1°C. Strontium incorporation into statoliths is also inversely affected by temperature, but there was a significant positive effect of temperature on Sr incorporation into protoconch. These data suggest larval statoliths and protoconchs can meaningfully record variation in seawater physical and chemical properties, and, hence, have potential as natural tags of natal origin. *Copyright © 2003 Elsevier Ltd*

1. INTRODUCTION

Examination of the trace metal content of biogenic carbonates (e.g., foraminiferal shell calcite, coral aragonite) provides a wealth of information about the chemistry of both historic and modern oceanic seawater. Historic information about climate change (Lea et al., 2000), oceanic nutrient geochemistry (Lea et al., 1989), deep-ocean circulation patterns (Adkins et al., 1998; Boyle, 1990), histories of anthropogenic metal pollution (Schettler and Pearce, 1996; Price and Pearce, 1997), and reconstructed patterns in El Niño Southern Oscillations (Shen and Sanford, 1990; Tudhope et al., 2001) can all be elucidated from carbonate-bound trace metals.

Recently, fish biologists have found that the trace element composition of aragonitic fish otoliths (ear stones) is also useful for reconstructing fish environmental history. As fish migrate or disperse across gradients in seawater temperature, salinity, or elemental composition, their travels can be 'recorded' as changes in the chemical composition of their hard parts. Fish scientists have examined trace elements present in the otolith to track migration and dispersal patterns, and to identify spawning grounds and juvenile nursery habitats (Gillanders and Kingsford, 1996; Campana, 1999; Swearer et al., 1999; Thorrold et al., 2001). Perhaps most useful from a fisheries perspective is that larval otoliths formed at the source of production potentially carry a natural chemical tag of their origin in their elemental composition. This natural tag can represent a permanant record of a fish's natal origin, and can later be sampled in juvenile and adult individuals by laser ablation techniques. Analogous tools exist for identifying invertebrate larval natal origin, yet their utility has only recently been investigated (Dibacco and Levin, 2000; Zacherl, 2002; Zacherl et al., 2003). Larval invertebrate molluscs, for example, form aragonitic statoliths and protoconchs (larval shells) that might also record a natural natal tag. For both fishes and invertebrates, development of this tool, leading to identification of source populations, would greatly enhance the ability of resource managers to effectively manage fishery resources (Crowder et al., 2000; Warner et al., 2000).

Using the trace elemental composition of larval aragonitic otoliths, statoliths, and protoconchs as a proxy for natal source relies on the assumption that spatial variation in seawater physical and chemical properties will somehow be reflected in the elemental composition of the larval hard part. The extent of trace metal substitution into otolith, statolith, and protoconch aragonite structures could be influenced by a host of potential factors including dissolved ion concentrations in seawater, thermodynamic constraints on ion substitution, temperature, salinity, and precipitation rate. Further, potential fractionation of ions as they move across interfaces from water to gills, and from blood to extrapallial or endolymph fluid, can complicate correlations between water and carbonate chemistry (Campana, 1999).

The mechanism of metal substitution into calcified structures is understood as follows: divalent metals like Sr 2++ and Ba 2++ have ionic radii similar to Ca 2++ and can therefore be incorporated into calcified structures such as aragonite through substitution reactions, e.g.,

$$CaCO_3 + Ba^{2+} \rightarrow BaCO_3 + Ca^{2+} \quad (1)$$

Given the long list of factors potentially affecting the incorporation of metals into aragonite, the most parsimonious way to relate seawater metal/Ca (Me/Ca) directly to aragonite Me/Ca

* Author to whom correspondence should be addressed. *Present address:* Department of Biological Science (MH-282), California State University, Fullerton, CA 92834-6850 (dzacherl@fullerton.edu).

is to determine it empirically. Lea and Spero (1992) discuss a method to relate seawater Me/Ca to carbonate Me/Ca by the expression

$$[Me/Ca]_{carbonate} = D_{Me}[Me/Ca]_{H_2O} \quad (2)$$

where D_{Me} is an empirical partition coefficient that directly relates observed carbonate Me/Ca to the total ion ratios in seawater.

In some biogenic carbonates, and for some elements, the relationship between seawater metal/Ca and carbonate metal/Ca has been validated empirically. For example, Lea and Spero (1992, 1994) and Mashiotta et al. (1997) determined partition coefficients for Ba and Cd in shell calcite of planktonic Foraminifera via controlled lab culturing experiments. Bath et al. (2000) and Wells et al. (2000) completed culturing experiments on fishes to determine partition coefficients of trace metals in otolith aragonite (Sr, Ba) and scale apatite (Sr, Cd, Ba).

For ocean dwelling species forming calcified structures, variations in Sr/Ca and Mg/Ca cannot easily be explained by examining variations in seawater Me/Ca because Sr/Ca and Mg/Ca ratios are nearly constant in oceanic seawater (i.e., Sr and Mg are generally considered conservative elements, but see de Villiers, 1999). Environmental factors such as temperature likely explain much of the Mg/Ca variation seen in biogenic carbonates (Nürnberg et al., 1996; Lea et al., 1999). However, there is a rich history of contradiction in the literature concerning Sr incorporation into biogenic carbonates as a function of temperature. Lea et al. (1999) provide empirical evidence that Sr/Ca increases with temperature in foraminiferal calcite. However, correlative field studies on coral aragonite generally demonstrate an inverse effect of temperature (de Villiers et al., 1995; Shen et al., 1996; Marshall and McCulloch, 2002). This inverse effect of temperature on Sr/Ca in aragonite concurs with thermodynamic predictions (Appendix 1) and with studies on inorganic precipitation of aragonite (Kinsman and Holland, 1969). It is not alarming that metal incorporation into calcite versus its polymorph, aragonite, shows differing responses to temperature. However, contradictions exist even within aragonite studies. Empirical laboratory studies have reported positive (Bath et al., 2000), negative (Smith et al., 1979; Secor et al., 1995), nonlinear (Kalish, 1989; Elsdon and Gillanders, 2002) and nonexistent (Gallahar and Kingsford, 1996) relationships between temperature and Sr/Ca in aragonite coral and otolith.

To date, only one study has examined factors influencing trace metal uptake into statolith aragonite (Ikeda et al., 2002); no study has examined factors influencing trace metal uptake into protoconch aragonite. In this study, we test the assumption that spatial variation in the physical and chemical properties of seawater can be reflected in the elemental composition of aragonitic statoliths and shells from marine invertebrates. Under controlled culturing conditions, we examine the incorporation of Ba and Sr into the protoconch and statolith aragonite of encapsulated *Kelletia kelletii* larvae as a function of temperature, and further examine the incorporation of Ba as a function of seawater Ba/Ca. We comment upon the utility of these invertebrate hard parts as markers of natal origin.

Table 1. Summary of average seawater Ba/Ca μmol/mol ±1 standard error for each seawater Ba/Ca treatment group. N = 6 water samples per treatment.

Treatment level	Avg. seawater Ba/Ca (μmol/mol) ± 1 SE
Ambient	3.47 ± 0.03
2×	6.31 ± 0.02
4×	11.78 ± 0.10
6×	17.49 ± 0.08

2. EXPERIMENTAL METHODS

2.1. Study Organism

Kelletia kelletii is a common predatory buccinid gastropod in rocky subtidal habitats from Baja California, Mexico to central California, USA. Juveniles and adults generally occupy a vertical distribution from 2 to 70 m in depth (Rosenthal, 1970) and typically occur on rocky reefs and cobble-sand interfaces in kelp forests. This whelk is a generalist predator that feeds on a variety of mobile and sessile invertebrates.

Kelletia kelletii reproduce annually, with egg laying restricted to late spring and summer (late May through August). The females lay egg capsules in masses on benthic hard substrate where embryos develop into encapsulated veliger larvae for a period of approximately 30–34 d. Each egg capsule contains approximately 400–2000 larvae. The hatched veliger larvae are pelagic; the length of this life stage is unknown (Rosenthal, 1970; Morris et al., 1980).

2.2. Larval Culturing

SCUBA divers collected egg capsules from masses produced by *Kelletia kelletii* at Isla Vista Reef, Santa Barbara, CA, in early July 2000. We rinsed egg capsules with 0.2 μm filtered seawater to remove sand fragments and algal growth, then added 4 egg capsules each to 24 culture flasks, randomizing brood stock identification. Groups of three flasks were randomly assigned to each of four levels of seawater Ba/Ca at two treatment temperatures. The Ba/Ca treatment groups included a baseline treatment at ambient coastal seawater Ba/Ca, and then 2×, 4×, and 6× ambient levels (see Table 1 for Ba/Ca values). Ba concentrations ranged from ~ 35 nmol/L (ambient) to 176 nmol/L, approximating the actual range present in the world oceans (Chan et al., 1977; Ostlund et al., 1987). Sr concentrations were not manipulated because this species inhabits oceanic waters, where Sr varies by only 2–3% globally (de Villiers, 1999). The temperature treatment groups (11.4 and 17.1°C) reflected the average extremes in temperature throughout *K. kelletii*'s range during larval development periods in June through August. Seawater temperature was controlled by partially immersing culture flasks into water baths equipped with heaters and chillers. Tidbit temperature loggers recorded water temperature within each water bath every 14 min throughout the entire experiment (Table 2). For the culturing water source, 100 L of 0.2 μm filtered ambient seawater (collected from running seawater pipes at University of California, Santa Barbara) were archived into acid leached carboys. The Ba spiked seawater was prepared by adding appropriate amounts of a stock solution of $BaCl_2$ into acid leached Nalgene bottles and then adding these prepared treatments to the culturing flasks. We collected

Table 2. Summary of temperature (T) conditions for cultures in the warm and cold temperature treatment groups.

Variable	Warm treatment	Cold treatment
Mean T (°C)	17.1	11.4
Standard deviation	0.2	0.2
Minimum T	16.5	10.9
Maximum T	17.6	12.2
Count	3393	3393

water samples from each prepared treatment level every fourth day of the experiment just before introduction into culturing flasks. Samples were filtered through 0.2 μm membrane filters, acidified with trace metal grade 12 N HCL to ~ pH2, and then stored for analysis (Table 1). We changed 50% of the volume of each culture flask every other day to maintain water quality. The culturing experiment ran until larvae were near hatching for a total of 30 d. At termination, we collected water samples from each culturing flask to ensure that seawater Ba and Sr concentrations remained constant among culture flasks within a treatment group. In all cases, there were no significant differences in seawater Ba/Ca or Sr/Ca among flasks. Further, the Sr concentrations remained constant among all treatment groups.

2.3. Protoconch, Statolith, and Water Analyses

At termination of the experiment, we isolated larval statoliths and protoconchs for analysis. All of the isolation steps were performed in a clean laboratory equipped with class 100 laminar flow hoods. All of the glassware used in the isolation steps was first cleaned using Citranox soap, rinsed 5 times with distilled water (resistivity >2 M$\Omega \cdot$ cm) and then rinsed 5 times with ultra pure water (resistivity >18.1 M$\Omega \cdot$ cm).

To isolate protoconchs from the encapsulated veliger larvae, we removed the larvae from the capsules and dissolved all visible organic tissue away from the shells in an acid rinsed glass beaker using a peroxide cleaning solution of an equal volume mixture of 30% H_2O_2 buffered in 0.1 N NaOH. Protoconch and statolith material could be separated using a 50μm mesh filter, and the protoconchs were then rinsed 5 times with ultra pure water (resistivity >18.1 M$\Omega \cdot$ cm). To ensure sufficient shell material for trace element analysis, protoconchs from individual larval snails within a capsule were pooled into groups of 50 and then dry stored in ultra pure H_2O rinsed polyethylene vials. To remove any remaining organics from the protoconchs, we cleaned each sample using 250 μL 15% H_2O_2 in 0.05 N NaOH for 20 min at 65°C, then rinsed each sample 4 times with ultra pure H_2O, heat rinsed them with ultra pure H_2O for 20 min at 65°C, and then rinsed them again with ultra pure H_2O. Using a small amount of ultra pure H_2O, we transferred samples into acid-leached polyethylene vials, and completely dissolved the samples in 400 μL 0.1 N nitric acid spike solution containing enriched ^{135}Ba, scandium 45 (^{45}Sc) and yttrium 89 (^{89}Y). These isotope spikes are used to quantify the concentrations of Ba by isotope dilution analysis (Lea and Martin, 1996), and Ca and Sr by means of internal standardization equations. Samples were blocked by treatment group, such that one sample from each treatment comprised a block within which samples were randomized. These samples were introduced into a Finnigan Element 2 sector field inductively coupled plasma mass spectrometer (ICP-MS) using a microflow nebulizer at 20 μL/min. Sensitivity measured 10^6 cps for 1 ppb indium. We formulated a mock shell solution that mimicked the Ba/Ca and Sr/Ca ratios expected in molluscan aragonite (~ 2 μmol/mol and ~ 9 mmol/mol, respectively). This reference material could then be used to determine the precision of the solution-based analysis. The mock shell consistency standard was analyzed twice at the beginning of the experimental run and twice at the termination of the run. The reproducibility of the mock shell consistency standard during the experimental run was 0.71% for Ba and 0.94% for Sr (n = 6). Detection limits were calculated for each isotope by calculating the standard deviation of the intensities of representative isotopes present in 1% nitric acid (HNO_3)instrument blanks, and then multiplying the standard deviation by three. Intensities of blank subtracted samples were >2000 times the detection limit for Ba and >1000 times the detection limit for Ca and Sr. Ba and Sr concentrations were standardized to Ca. We compared larval protoconch Ba/Ca and Sr/Ca using ANOVA to test for the hypotheses of no overall effect of seawater Ba/Ca on Ba incorporation into protoconch aragonite, no overall effect of temperature on Ba and Sr incorporation into protoconch aragonite, and no interaction effect between temperature and seawater Ba/Ca on Ba incorporation into protoconch aragonite.

We collected water samples for each treatment every 4 d and additionally collected water samples from randomly selected culture bottles when changing seawater, for a total of 6–8 seawater samples per treatment. Water samples were analyzed using isotope dilution ICP-MS for Ba and internal standardization procedures for Sr and Ca.

To isolate larval statoliths from the egg capsules, we removed the larvae from the capsules and released the statoliths by immersing the larvae into a peroxide cleaning solution of 15% H_2O_2 in 0.05 N NaOH. Released statoliths would fall to the bottom of the glass beaker. After vigorously swirling the beaker to concentrate the statoliths in the center, they were collected with a pipette. We pipetted statoliths into a glass beaker containing 15–20 mL ultra pure H_2O to rinse the cleaning solution away, then repeated this rinse step. Statoliths were again collected into the center of the glass beaker, and then pipetted onto an ultra pure H_2O rinsed 20×20 mm plastic slide. We used an acid rinsed pipette tip to draw off excess water, and allowed the remaining water to evaporate in a class 100 clean hood. Statoliths were mounted onto double-sided tape (Scotch) for laser ablation ICP-MS analysis. To measure Ba/Ca and Sr/Ca ratios in larval statoliths, we analyzed 10 individual larval statoliths per culture. We introduced samples into the ICP-MS using a VG-UV microprobe Nd:YAG laser ablation system, frequency-quadrupled to 266 nm with a crater diameter of 20 μm. Each statolith was completely consumed in ablation. In our system, we directly connected the carrier gas line from the laser sample cell to the nebulizer system of the ICP-MS. When samples were being ablated by the laser and transferred to the spray chamber, the nebulizer was aspirating a 1% HNO_3 solution. Similarly, when standard solutions in a 1% HNO_3 matrix and 1% HNO_3 instrument blanks were aspirated through the nebulizer, the carrier gas from the sample cell flowed. In this manner, the plasma conditions were kept constant during analysis of standards, instrument blanks and samples. The Me/calcium ratio was determined using matrix matched solution based standards of known Me/calcium ratio and applying a mass bias correction (Rosenthal et al., 1999). We used National Institute of Standards and Technology (NIST-612) glass standards as reference materials from which we could estimate the precision of the laser ablation method. The reproducibility of the Ba/Ca ratios in the NIST-612 standard for this study was 3.3%. We chose to quantify elemental concentrations using our matrix matched standard solution instead of the NIST standard, since the NIST glass lacks the aragonite-dominated matrix of statoliths. This semi-quantitative approach is not without its limitations. Despite evidence of good quantitative agreement between aragonite-dominated matrix matched materials analyzed in solution versus laser-based modes (Thorrold et al., 1997), which would suggest that our use of solution based standards is robust, the continued lack of certified matrix matched solid reference materials means that comparisons among other published studies should be interpreted with caution (Campana, 1999). We again determined detection limits for each element using the method described above. Intensities of blank subtracted samples were >45 times the detection limit for Ba and >165 times the detection limit for Ca and Sr. We compared larval statolith Ba/Ca ratios using a nested ANOVA (statoliths nested within cultures, with statoliths assigned a random effect) to test for the hypotheses of no overall effect of seawater Ba/Ca on Ba incorporation into statolith aragonite, no overall effect of temperature on Ba incorporation into statolith aragonite, and no interaction effect between temperature and seawater Ba/Ca on Ba incorporation into statolith aragonite. Larval statolith Sr/Ca ratios were compared using a nested ANOVA (statoliths nested within cultures, with statoliths assigned a random effect) to test for the hypothesis of no overall effect of temperature on Sr incorporation into statolith aragonite.

3. RESULTS

3.1. Ba/Ca in Protoconchs

The Ba/Ca ratios in protoconchs from encapsulated *Kelletia kelletii* larvae were directly proportional to the Ba/Ca in the culturing seawater (Fig. 1, Table A1). We log normalized the Ba/Ca protoconch data to correct for heteroscedasticity in error variance, and then analyzed the data by ANOVA. The ANOVA showed a significant temperature effect and a significant effect of seawater Ba/Ca on log Ba/Ca in protoconch (Table A2 for test statistics details).

At 11.4°C, least squares regression describes a tight linear

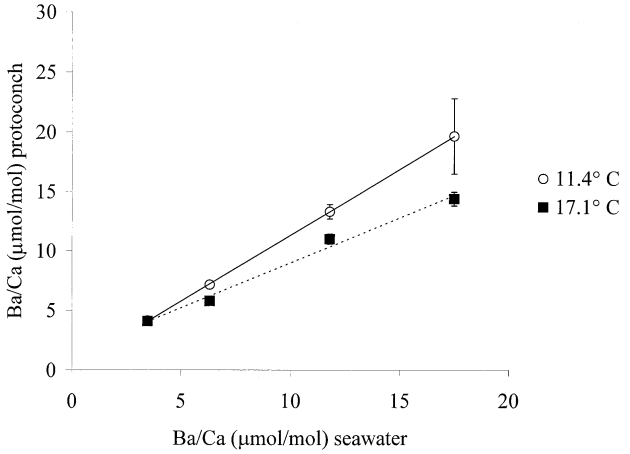

Fig. 1. Mean Ba/Ca ratios ($[Ba/Ca]_{protoconch} \pm SE$) in protoconchs of laboratory-reared larval *Kelletia kelletii* versus Ba/Ca ratios of culturing water ($[Ba/Ca]_{H_2O} \pm SE$) at 11.4°C (o, solid line) and at 17.1°C (solid square, dashed line). Lines show linear least squares regressions for both temperature treatments. At 11.4°C, the linear relationship ($r^2 = 0.94$, $p < 0.0001$) is $[Ba/Ca]_{protoconch} = 1.11 \pm 0.23\ [Ba/Ca]_{H_2O} + 0.22 \pm 2.33$. At 17.1°C, the linear relationship ($r^2 = 0.98$, $p < 0.0001$) is $[Ba/Ca]_{protoconch} = 0.76 \pm 0.10\ [Ba/Ca]_{H_2O} + 1.41 \pm 1.02$.

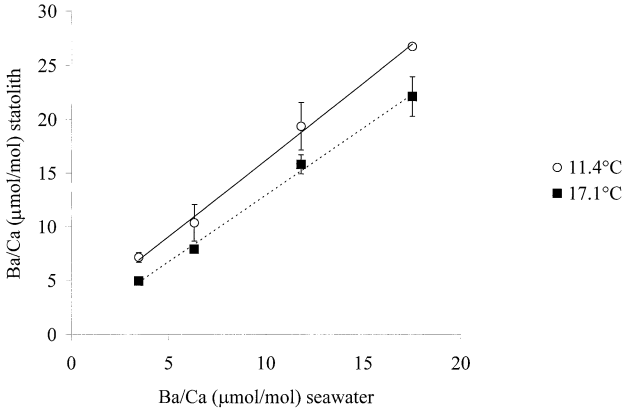

Fig. 2. Mean Ba/Ca ratios ($[Ba/Ca]_{statoliths} \pm SE$) in statoliths of laboratory-reared larval *K. kelletii* versus Ba/Ca ratios of culturing water ($[Ba/Ca]_{H_2O} \pm SE$) at 11.4°C (o, solid line) and at 17.1°C (solid square, dashed line). Lines show linear least squares regressions for both temperature treatments. At 11.4°C, the linear relationship ($r^2 = 0.93$, $p < 0.0001$) is $[Ba/Ca]_{statolith} = 1.43 \pm 0.27\ [Ba/Ca]_{H_2O} + 1.91 \pm 3.01$. At 17.1°C, the linear relationship ($r^2 = 0.95$, $p < 0.0001$) is $[Ba/Ca]_{statolith} = 1.25 \pm 0.20\ [Ba/Ca]_{H_2O} + 0.43 \pm 2.24$.

relationship ($r^2 = 0.94$, $p < 0.0001$) between $[Ba/Ca]_{protoconch}$ and $[Ba/Ca]_{H2}O$ as:

$$[Ba/Ca]_{protoconch} = 1.11 \pm 0.23\ [Ba/Ca]_{H_2O} + 0.22 \pm 2.33 \quad (3)$$

At 17.1°C, the linear relationship ($r^2 = 0.98$, $p < 0.0001$) was:

$$[Ba/Ca]_{protoconch} = 0.76 \pm 0.10\ [Ba/Ca]_{H_2O} + 1.41 \pm 1.02 \quad (4)$$

The errors associated with the regression coefficients reported above (and hereafter) represent 95% confidence intervals.

To calculate partition coefficients (D_{Ba}), the convention is to force the regression lines through the zero intercept (Lea and Spero, 1992, 1994), with the assumption that larval molluscs developing in Ba free seawater would be expected to have no Ba in their statoliths and protoconchs. This convention makes the assumption that $[Ba/Ca]_{protoconchs}$ reflects only Ba contributions from seawater and precludes the potential for maternal Ba contributions in yolk. In fish otoliths, the majority of Sr and Ca in the carbonate crystal are thought to be derived from water (Farrell and Campana, 1996); for Ba, the relative contributions from environment versus diet are unknown. Nonetheless, for the purposes of comparison with other studies, we proceeded with the convention of forcing the regression lines through the zero intercept to calculate D_{Ba}. Estimates of D_{Ba} were 1.13 ± 0.11 (95% CI) at 11.4°C and 0.88 ± 0.07 (95% CI) at 17.1°C.

3.2. Ba/Ca in Statoliths

The Ba/Ca ratios in statoliths from encapsulated *Kelletia kelletii* larvae were, like protoconch Ba/Ca, directly proportional to the Ba/Ca in the culturing seawater (Fig. 2, Table A1). Treatment group variances violated the ANOVA assumption of heteroscedasticity of variances; therefore, we log normalized the Ba/Ca protoconch data to complete the ANOVA. The ANOVA showed a significant temperature effect and a significant effect of seawater Ba/Ca on log Ba/Ca in statoliths (Table A3).

At 11.4°C, least squares regression describes a linear relationship ($r^2 = 0.93$, $p < 0.0001$) between $[Ba/Ca]_{statolith}$ and $[Ba/Ca]_{H_2O}$ as:

$$[Ba/Ca]_{statolith} = 1.43 \pm 0.27\ [Ba/Ca]_{H_2O} + 1.91 \pm 3.01 \quad (5)$$

At 17.1°C, the linear relationship ($r^2 = 0.95$, $p < 0.0001$) was:

$$[Ba/Ca]_{statolith} = 1.25 \pm 0.20\ [Ba/Ca]_{H_2O} + 0.43 \pm 2.24 \quad (6)$$

The errors associated with the regression coefficients reported above represent 95% confidence intervals. To calculate partition coefficients (D_{Ba}), we constrained the regression lines through the zero intercept (see section 3.1.) to calculate D_{Ba}. Estimates of D_{Ba} were 1.58 ± 0.13 (95%CI) at 11.4°C and 1.29 ± 0.09 (95% CI) at 17.1°C.

3.3. Sr/Ca in Protoconchs and Statoliths

Results from ANOVA demonstrate a positive effect of temperature on strontium incorporation into protoconch ($p = 0.0004$, Table A4). Protoconch Sr/Ca increased from 2.73 ± 0.06 (SE) mmol/mol at 11.4°C to 3.08 ± 0.06 mmol/mol at 17.1°C (Fig. 3).

For statoliths, treatment group variances violated the ANOVA assumption of heteroscedasticity of variances; therefore, we log normalized the Sr/Ca statolith data to complete the ANOVA. The ANOVA showed a significant inverse temperature effect on Sr incorporation into statoliths ($p = 0.001$, Table A5). Statolith Sr/Ca decreased from 10.16 ± 0.09 mmol/mol at 11.4°C to 9.11 ± 0.09 (SE) mmol/mol at 17.1°C (Fig. 3).

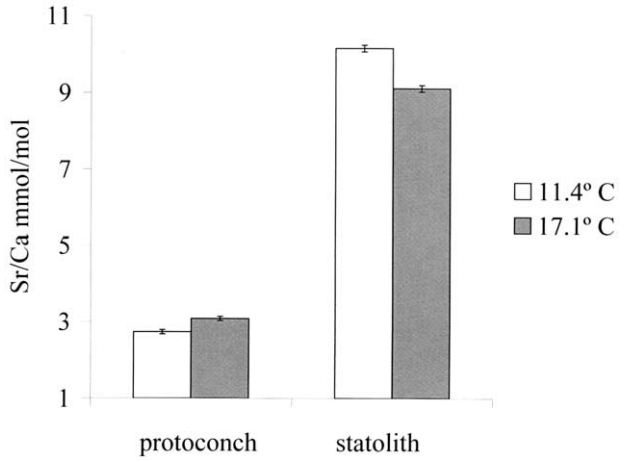

Fig. 3. Mean Sr/Ca ratios ($[Sr/Ca]_{hard\ part} \pm SE$) in protoconchs and statoliths of laboratory-reared larval *K. kelletii* at 11.4°C (open square) and at 17.1°C (solid square).

4. DISCUSSION

4.1. Ba Partition Coefficients in Biogenic Aragonitic Structures

Calculated partition coefficient values for Ba, ranging from 0.88 for protoconchs at 17.1°C to 1.58 for statoliths at 11.4°C, bracket D_{Ba} values previously calculated for the aragonitic skeletons of hermatypic corals (~1.3; Lea et al., 1989). However, these D_{Ba} values differ dramatically from those reported by Bath et al., (2000) in their culturing study examining Ba uptake into the aragonitic otoliths of estuarine fish larvae (~0.06). A partition coefficient less than 1.0, such as in the Bath et al., (2000) study, indicates that Ba is discriminated against during precipitation. This discrimination is probably not due to thermodynamic constraints, as Ba is readily incorporated into aragonite (Speer, 1983). Rather, the discrimination may be due to physiologic fractionation of ions as they move across fish membrane interfaces (Campana, 1999). The difference in their reported D_{Ba}value versus that for aragonitic structures in our study may simply reflect variation in physiologic fractionation of Ba ions.

Linear least squares regressions (as depicted in Figs. 1 and 2 for protoconchs and statoliths, respectively) indicate a lack of a convincing fit of the data through the origin. This nonzero value for protoconch and statolith Ba/Ca with zero Ba/Ca in seawater has also been observed in fish otolith culturing studies (Bath et al., 2000), but does not seem to be indicated by foraminifera culturing studies (e.g., Lea and Spero, 1992). There are several possible explanations for the observed pattern. First, these data might indicate a nonlinearity between seawater Ba/Ca and protoconch or statolith Ba/Ca at low seawater Ba concentrations. Alternatively, an additional source (e.g., yolk) besides seawater might contribute Ba to the developing larva as it builds its calcified larval structures. Last, while cleaning experiments using the methods described for this study suggest effective removal of the organic components of these carbonate materials (D. Zacherl, unpublished data), the possibility remains that some residual organic component of the protoconchs/statoliths contribute to the measured Ba/Ca ratio. Future studies aimed at measuring maternal contributions (i.e., from yolk) of elements may help account for this observed elevated Ba/Ca in larval calcified structures.

4.2. Temperature Effects on Ba and Sr Incorporation

Our results represent the first conclusive demonstration of a temperature effect on D_{Ba} into an aragonitic structure. Lea et al., (1989) speculated that temperature effects likely influenced quasiperiodic oscillations in coral aragonite Ba/Ca, but other studies do not appear to support this influence (e.g., Sinclair et al., 1998). In particular, Bath et al. (2000) examined Ba uptake into the aragonitic otoliths of marine fish under controlled laboratory culturing conditions, yet found no temperature effect. One possible explanation for the temperature effect found in *K. kelletii* aragonitic hard parts could be reflected in the partition coefficients that hover near the calculated thermodynamic distribution coefficient for Ba in aragonite (~1.3, Shen and Sanford, 1990). In other words, Ba/Ca in aragonitic *K. kelletii* structures appears to closely reflect seawater Ba/Ca, making Ba incorporation largely under the control of thermodynamic constraints. Thermodynamic calculations also predict a temperature effect. The reaction

$$Ba^{2+} + CaCO_3 \rightarrow BaCO_3 + Ca^{2+} \quad (7)$$

has a negative enthalpy (i.e., exothermic; Appendix 1); it should be favored at colder temperatures. Our higher D_{Ba} values at lower temperatures qualitatively fit predictions imposed by thermodynamic considerations.

Another explanation for our observed temperature effect on D_{Ba} may be related to aragonite crystal precipitation rate. The relationship between precipitation rate and barium incorporation into biogenic aragonite is relatively unexplored. The Bath et al. (2000) study suggests barium incorporation into aragonitic otoliths is unrelated to precipitation rate. Studies of synthetic aragonite growth concur with this notion that rate effects are not involved (Zhong and Mucci, 1989). In the absence of growth rate data from this culturing experiment and an experimental design that could decouple the effects of temperature and growth rate, the role of aragonite precipitation rate in determining Ba/Ca ratios in our statoliths and protoconchs is undetermined. We plan future culturing experiments aimed at teasing apart temperature effects and aragonite precipitation rate.

It was difficult to predict if we might expect a Sr-temperature relationship in this culturing experiment because of the history of contradiction in the literature concerning Sr incorporation into aragonite as a function of temperature. The opposite relationships found in this experiment are perplexing. Thermodynamic parameters predict a negative temperature dependence on Sr incorporation into aragonite structures (Appendix 1), which might explain the results for Sr in statoliths. However, protoconch Sr/Ca is clearly not under thermodynamic control.

What other factors could influence Sr/Ca in such a way as to reverse the Sr-temperature relationship observed in protoconch versus statolith? In coral aragonite studies, there is evidence that Sr incorporation is inversely proportional to coral extension (growth) rate (de Villiers et al., 1995). Stecher et al. (1996) reported opposing Sr-temperature relationships in studies of the

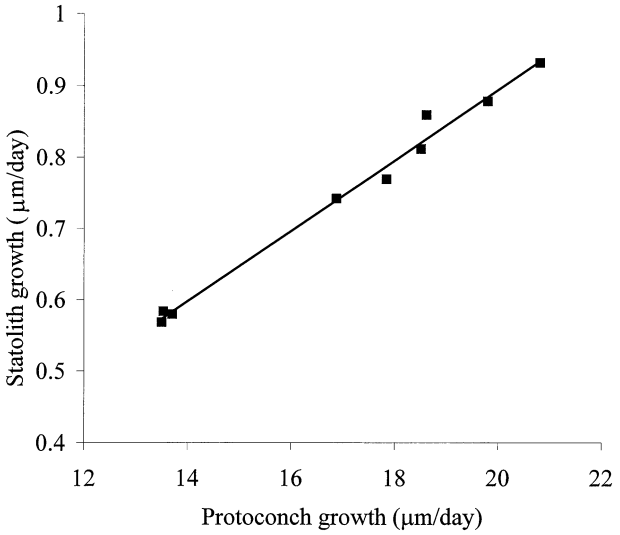

Fig. 4. Protoconch growth rate (μm/d) versus statolith growth rate (μm/d) in laboratory-reared larval *K. kelletii*, including linear regression line ($y = 0.05x - 0.09$, $r^2 = 0.99$).

aragonite layers of shells of two mollusk species. One species exhibited greatest growth during warm summer months, while the other exhibited greatest growth during cold winter months. Stecher et al. concluded that differences in growth rate provided a more parsimonious explanation than temperature for the differential patterns of Sr incorporation. To test whether that explanation could explain our pattern, we reared larvae at three temperatures and measured the growth rates of statolith and protoconch. Temperature had a positive effect on growth rates of both materials and the relationship between statolith and protoconch growth rates was strongly linear (Fig. 4). This evidence strongly suggests that the opposite Sr-temperature relationships we observed were not due to differences in the response of growth rate to temperature. However, the growth rates of these two materials did differ by more than an order of magnitude, with protoconch growing $\sim$ 20 times faster than statolith (Fig. 4). The possibility remains that the slope of the temperature effect reverses as growth rate increases. This explanation seems unlikely but cannot be ruled out without further experimentation.

Last, the absolute value of Sr/Ca in protoconchs is $\sim$1/3 that for Sr/Ca in statoliths (Fig. 3). Incorporation of Ba into protoconch versus statolith shows the same qualitative effect, where the absolute value of Ba/Ca in protoconch is $\sim$1/2 to 2/3 that for statoliths (at 11.4°C, compare D_{Ba} protoconch = 1.13 to D_{Ba} statolith = 1.58; at 17.1°C, compare D_{Ba} protoconch = 0.88 to D_{Ba} statolith = 1.29). This pattern, coupled with the observation of a positive temperature dependence for Sr/Ca into protoconch, which contradicts the thermodynamic predictions for Sr incorporation into aragonite, suggests possible strong biological control on protoconch Me/Ca. Elements follow dissimilar transport pathways from seawater to protoconch versus statolith. The pathway to statolith carries elements from seawater to blood plasma to statocyst endolymph. In contrast, the pathway to protoconch moves elements from seawater to blood plasma to the extrapallial fluid in the mantle. Differential Sr discrimination across dissimilar biological membranes in mantle versus statocyst may play a role in determining the opposing responses to temperature observed in protoconch versus statolith.

4.3. Statoliths and Protoconchs as Markers of Natal Origin

To utilize the larval portion of aragonitic structures as markers of natal origin, it is important to demonstrate that variation in seawater physical and chemical properties will be reflected in the elemental composition of the protoconch or statolith. In the case of Ba incorporation into *K. kelletii* larval hard parts, we demonstrated that Ba/Ca ratios would vary in a predictable way as a function of both seawater Ba/Ca and temperature.

The combined effect of colder temperatures and higher seawater Ba/Ca leading to higher aragonite Ba/Ca is the best possible outcome for this tool in the California borderland waters. The range of *K. kelletii* extends from Baja California, Mexico to Monterey, California, USA, a span where coastal oceanic conditions are characterized by dramatic shifts in upwelling and temperature regimes. Cold-water regions, such as those in the northern part of this species' range, are characterized by more frequent upwelling. Ba follows a nutrient-like profile in the oceans, and therefore will be enriched in upwelled waters (Chan et al., 1977). Larvae developing in the northern portions of the range should have enriched Ba/Ca ratios in protoconch and statolith relative to those formed in the warmer, more nutrient poor regions of the range. This prediction relies on the assumption that other factors that could affect Ba incorporation do not override the effects of seawater Ba/Ca and temperature. Preliminary survey work on *K. kelletii* protoconchs and statoliths from encapsulated veliger larvae collected from throughout the range of this species lends support to this prediction, with significantly higher Ba/Ca ratios at sites in the colder upwelling region of the north versus warm water sites (Zacherl, 2002).

Variation in temperature will also be reflected in the Sr/Ca ratios of the protoconch and statolith, but the Sr-temperature relationship is opposite for the two aragonite materials. We predict that statoliths formed in cold-water regions will show enriched Sr/Ca relative to those formed in warmer regions. The opposite pattern is predicted for protoconchs. As with the Ba/Ca patterns, preliminary survey work on *K. kelletii* protoconchs and statoliths from field-collected encapsulated larvae concurs with these predictions. Statoliths formed at sites in the colder region of the north showed significantly higher Sr/Ca versus those formed at warm water sites. Warm-water protoconchs has significantly higher Sr/Ca than cold-water protoconchs (Zacherl, 2002). While the mechanism controlling this pattern remains inexplicable, the pattern itself appears predictable.

5. SUMMARY

Kelletia kelletii larval statolith and protoconch Ba/Ca ratios vary positively with seawater Ba/Ca and inversely with temperature. Sr/Ca ratios in protoconch vary positively with temperature, while Sr/Ca ratios in statolith vary inversely with temperature. Our estimates of D_{Ba} for statoliths and protoconchs are close to Ba partition coefficient values for other

invertebrate aragonitic structures, such as coral skeletons. Because of the evident temperature effect, future studies with biogenic aragonite should focus on carefully calibrating the D_{Ba} values with respect to temperature. Our results suggest that trace elements in invertebrate statoliths and protoconchs reflect seawater chemical and physical properties and, hence, hold promise as tags of natal source.

Acknowledgments—This is contribution number 113 of the Partnership for Interdisciplinary Studies of Coastal Oceans (PISCO): A Long-Term Ecological Consortium funded by the David and Lucile Packard Foundation. This study is part of D. Zacherl's Ph.D. dissertation. She thanks Sigma Xi, and the Lerner-Gray Foundation for additional financial support and Bob Warner, Steve Gaines, and Armand Kuris for helpful comments on earlier versions of this manuscript. We further wish to thank Simon Thorrold and two anonymous reviewers for thoughtful comments on the original manuscript. The purchase and installation of the Element 2 at UCSB was partly funded by the National Science Foundation under Grant OCE-9906821 (D.W.L.).

Associate editor: R. Burdige

REFERENCES

Adkins J. F., Cheng, H., Boyle E. A., Druffel E. R. M., and Edwards R. L. (1998) Deep-sea coral evidence for rapid change in ventilation of the deep North Atlantic 15,400 years ago. *Science* **280**, 725–728.

Bath G. E., Thorrold S. R., Jones C. M., Campana S. E., McLaren J. W., and Lam J. W. H. (2000) Sr and Ba uptake in aragonitic otoliths of marine fish. *Geochim. Cosmochim. Acta* **64**, 1705–1714.

Boyle E. A. (1990) Quaternary deepwater paleoceanography. *Science* **249**, 863–870.

Busenberg E. and Plummer L. N. (1986) The solubility of $BaCO_3$(cr) (witherite) in CO_2-H_2O solutions between 0 and 90°C, evaluation of the association constants of $BaHCO_3^+$ (aq) and $BaCO_3^0$ (aq) between 5 and 80°C, and a preliminary evaluation of the thermodynamic properties of Ba^{2+}(aq). *Geochim. Cosmochim. Acta* **50**, 2225–2233.

Campana S. E. (1999) Chemistry and composition of fish otoliths: Pathways, mechanisms and applications. *Mar. Ecol. Prog. Ser.* **188**, 263–297.

Chan L. H., Drummond D., Edmund J. M., and Grant B. (1977) On the barium data from the Atlantic GEOSECS expedition. *Deep-Sea Res.* **24**, 613–649.

Crowder L. B., Lyman S. J., Figueira W. F., and Priddy J. (2000) Source-sink population dynamics and the problem of siting marine reserves. *Bull. Mar. Sci.* **66**, 799–820.

de Villiers S. (1999) Seawater strontium and Sr/Ca variability in the Atlantic and Pacific oceans. *Earth Planet. Sci. Lett.* **171**, 623–634.

de Villiers S., Nelson B. K., and Chivas A. R. (1995) Biological controls on coral Sr/Ca and delta-O-18 reconstructions of sea surface temperatures. *Science* **269**, 1247–1249.

DiBacco C. and Levin L. A. (2000) Development and application of elemental fingerprinting to track the dispersal of marine invertebrate larvae. *Limnol. Oceanogr.* **45**, 871–880.

Drever J. I., ed. (1997) *The Geochemistry of Natural Waters: Surface and Groundwater Environments.* 3rd ed. Prentice-Hall.

Elsdon T. S. and Gillanders B. M. (2002) Interactive effects of temperature and salinity on otolith chemistry: Challenges for determining environmental histories of fish. *Can. J. Fish. Aquat. Sci.* **59**, 1796–1808.

Farrell J. and Campana S. E. (1996) Regulation of calcium and strontium deposition on the otoliths of juvenile tilapia *Oreochromis niloticus*. *Comp. Biochem. Physiol.* **115**, 103–109.

Gagan M. K., Ayliffe L. K., Beck J. W., Cole J. E., Druffel E. R. M., Dunbar R. B., and Schrag D. P. (2000) New views of tropical paleoclimates from corals. *Quat. Sci. Rev.* **19**, 45–64.

Gallahar N. K. and Kingsford M. J. (1996) Factors influencing Sr/Ca ratios in otoliths of *Girella elevata*: An experimental investigation. *J. Fish Biol.* **48**, 174–186.

Garrels R. M. and Christ C. L. (1965) *Solutions, Minerals, and Equilibria*. Freeman, Cooper.

Gillanders B. M. and Kingsford M. J. (1996) Elements in otoliths may elucidate the contribution of estuarine recruitment to sustaining coastal reef populations of a temperate reef fish. *Mar. Ecol. Prog. Ser.* **141**, 13–20.

Ikeda Y., Okazaki J., Sakurai Y., and Sakamoto W. (2002) Periodic variation in Sr/Ca ratios in statoliths of the Japanese Common Squid *Todarodes pacificus Steenstrup*, 1880 (Cephalopoda: Ommastrephidae) maintained under constant water temperature. *J. Exp. Mar. Biol. Ecol.* **273**, 161–170.

Kalish J. M. (1989) Otolith microchemistry: Validation of the effects of physiology, age and environment on otolith composition. *J. Exp. Mar. Biol. Ecol.* **132**, 151–178.

Kinsman D. J. J. and Holland H. D. (1969) The co-precipitation of cations with $CaCO_3$-IV. The co-precipitation of Sr^{2+} with aragonite between 16°C and 96°C. *Geochim. Cosmochim. Acta* **33**, 1–17.

Lea D. W., Shen G. T., and Boyle E. A. (1989) Coralline barium records temporal variability in equatorial Pacific upwelling. *Nature* **340**, 373–376.

Lea D. W. and Spero H. J. (1992) Experimental determination of barium uptake in shells of the planktonic Foraminifera *Orbulina universa* at 22°C. *Geochim. Cosmochim. Acta* **56**, 2673–2680.

Lea D. W. and Spero H. J. (1994) Assessing the reliability of paleochemical tracers: Barium uptake in the shells of planktonic foraminifera. *Paleoceanography* **9**, 445–452.

Lea D. W. and Martin P. A. (1996) A rapid mass spectrometric method for the simultaneous analysis of barium, cadmium, and strontium in Foraminifera shells. *Geochim. Cosmochim. Acta* **60**, 3143–3149.

Lea D. W., Mashiotta T. A., and Spero H. J. (1999) Controls on magnesium and strontium uptake in planktonic foraminifera determined by live culturing. *Geochim. Cosmochim. Acta* **63**, 2369–2379.

Lea D. W., Pak D. K., and Spero H. J. (2000) Climate impact of late quaternary equatorial Pacific sea surface temperature variations. *Science* **289**, 1719–1724.

Marshall J. F. and McCulloch M. T. (2002) An assessment of the Sr/Ca ratio in shallow water hermatypic corals as a proxy for sea surface temperature. *Geochim. Cosmochim. Acta* **66**, 3262–3280.

Mashiotta T. A., Lea D. W., and Spero H. J. (1997) Experimental determination of cadmium uptake in shells of the planktonic foraminifera *Orbulina universa* and *Globigerina bulloides*: Implications for surface water paleoreconstructions. *Geochim. Cosmochim. Acta* **61**, 4053–4065.

Morris R. H., Abbott D. P., and Haderlie E. C. (1980) In *Prosobranchia: Marine Snails.* p. 286. Intertidal Invertebrates of California. Stanford University Press.

Nürnberg D., Bigma J., and Hemleben C. (1996) Assessing the reliability of magnesium in foraminiferal calcite as a proxy for water mass temperatures. *Geochim. Cosmochim. Acta* **60**, 803–814.

Ostlund H. G., Craig H., Broeker W. S., and Spencer D. W. (1987) *GEOSECS Atlantic, Pacific, and Indian Ocean Expeditions.* Vol. 7, *Shore-Based Data and Graphics.* U.S. National Science Foundation.

Price G. D. and Pearce N. J. G. (1997) Biomonitoring of pollution by *Cerastoderma edule* from the Br. Isles: A laser ablation ICP-MS study. *Mar. Poll. Bull.* **34**, 1025–1031.

Rimstidt J. D., Balog A., and Webb J. (1998) Distribution of trace elements between carbonate minerals and aqueous solutions. *Geochim. Cosmochim. Acta* **62**, 1851–1863.

Rosenthal R. J. (1970) Observations on the reproductive biology of the Kellet's Whelk. *Kelletia kelletii. Veliger.* **12**, 319–324.

Rosenthal Y., Field M. P., and Sherrell R. M. (1999) Precise determination of element/calcium ratios in calcareous samples using sector field inductively coupled plasma mass spectrometry. *Anal. Chem.* **71**, 3248–3253.

Schettler G. and Pearce N. J. G. (1996) Metal pollution recorded in extinct *Dreissena polymorpha* communities, Lake Breitling, Havel Lakes System, Germany—A laser ablation inductively coupled plasma mass spectrometry study. *Hydrobiologia* **317**, 1–11.

Secor D. H., Henderson-Arzapalo A., and Piccoli P. M. (1995) Can otolith microchemistry chart patterns of migration and habitat utilization in anadromous fishes? *J. Exp. Mar. Biol. Ecol.* **192**, 15–33.

Shen G. T. and Sanford C. L. (1990) Trace element indicators of climate variability in reef-building corals. In *Global Ecological*

Consequences of the 1982–83 El Niño–Southern Oscillation (ed. P. W. Glynn), pp. 255–283. Elsevier.

Shen C. C., Lee T., Chen C. Y., Wang C. H., Dai C. F., and Li L. A. (1996) The calibration of $D^{[Sr/Ca]}$ versus sea surface temperature relationship for Porites corals. *Geochim. Cosmochim. Acta* **60**, 3849–3858.

Sinclair D. J., Kinsley L. P. J., and McCulloch M. T. (1998) High resolution analysis of trace elements in corals by laser ablation ICP-MS. *Geochim. Cosmochim. Acta* **62**, 1889–1901.

Smith S. V., Buddemeier R. W., Redalje R. C., and Houck J. E. (1979) Strontium-calcium thermometry in coral skeletons. *Science* **204**, 404–407.

Speer J. A. (1983) Crystal chemistry and phase relations of orthorhombic carbonates. In *Carbonates: Mineralogy and Chemistry* (ed. R. J. Reeder), pp. 145–190., Mineralogical Society of America.

Stecher H. A. III, Krantz D. E., Lord C. J. III, Luther G. W. III, and Bock K. W. (1996) Profiles of strontium and barium in *Mercenaria mercenaria* and *Spisula solidissima* shells. *Geochim. Cosmochim. Acta* **60**, 3445–3456.

Swearer S. E., Caselle J. E., Lea D. W., and Warner R. R. (1999) Larval retention and recruitment in an island population of a coral reef fish. *Nature* **402**, 799–802.

Thorrold S. R., Jones C. M., and Campana S. E. (1997) Response of otolith microchemistry to environmental variations experienced by larval and juvenile Atlantic croaker (*Micropogonias undulatus*). *Limnol. Oceanogr.* **42**, 102–111.

Thorrold S. R., Latkoczy C., Swart P. K., and Jones C. M. (2001) Natal homing in a marine fish metapopulation. *Science* **29**, 297–299.

Tudhope A. W., Chilcott C. P., McCulloch M. T., Cook E. R., Chappell J., Ellam R., Lea D. W., Lough J. M., and Shimmield G. B. (2001) Variability in the El Nino–Southern oscillation through a glacial–interglacial cycle. *Science* **291**, 1511–1517.

Warner R. R., Swearer S. E., and Caselle J. E. (2000) Larval accumulation and retention: Implications for the design of marine reserves and essential fish habitat. *Bull. Mar. Sci.* **66**, 821–830.

Wells B. K., Bath G. E., Thorrold S. E., and Jones C. M. (2000) Incorporation of strontium, cadmium, and barium in juvenile spot (Leiostomus xanthurus) scales reflects water chemistry. *Can. J. Fish. Aquat. Sci.* **57**, 2122–2129.

Zacherl D. C. (2002) Dispersal of larval invertebrates: Use of natural tags to identify natal origins. Ph.D. dissertation. University of California, Santa Barbara.

Zacherl D. C., Manríquez P. H., Paradis G., Day R. W., Castilla J. C., Warner R. R., Lea D. W., and Gaines S. G. (2003) Trace elemental fingerprinting of gastropod statoliths to study larval dispersal trajectories. *Mar. Ecol. Prog. Ser.* **248**, 297–303.

Zhong S. and Mucci A. (1989) Calcite and aragonite precipitation from seawater solutions of various salinities: Precipitation rates and overgrowth composition. *Chem. Geol.* **78**, 283–299.

APPENDIX 1

Exothermic reactions are favored at colder temperatures. For the reaction

$$Ba^{2+} + CaCO_3 \rightarrow BaCO_3 + Ca^{2+} \quad (01)$$

we calcuated the enthalpy change ($\Delta H°$) using the formula:

$$\begin{aligned}\Delta H°(\text{kJ/mol}) &= \text{H products} - \text{H reactants}\\ &= \Delta H°\,(Ca^{2+} + BaCO_3) - \Delta H°\,(Ba^{2+} + CaCO_3)\\ &= (-542.8 + -1210.9) - (-1206.4 + -532.5)\\ \Delta H° &= -14.8\ \text{kJ/mol}\end{aligned}$$

We obtained $\Delta H°$ values for Ba^{2+} and $BaCO_3$ from (Busenberg and Plummer 1986). The Ca^{2+} and $CaCO_3$ (aragonite)$\Delta H°$ values came from Drever (1997).

For any reaction with an associated enthalpy change, there will be temperature sensitivity, as shown by the van't Hoff equation (Garrels and Christ, 1965):

$$d\ln K/[d(1/T)] = -\Delta H/R \quad (02)$$

where T is temperature in Kelvin, R the gas constant, and K the equilibrium constant for the reaction. This equation predicts that the Ba/Ca content of a thermodynamically ideal aragonite will decrease by ~2.2% per degree between 0° and 30°C as determined by fitting an exponential relationship to the predicted relationship between K and T.

The difference in average temperature between treatment groups equals 5.7°C (17.1–11.4, from Table 1). A 5.7°C decrease in temperature predicts a ~13% increase in Ba/Ca. Results from this study demonstrate that with the 5.7°C decrease in temperature, Ba/Ca increased between 17 and 30% for both protoconch and statolith, except for protoconch at ambient Ba/Ca levels, where the increase measured only 1.4%. Overall, these results suggest at least partial thermodynamic control on protoconch and statolith Ba/Ca.

Using the same equation as above for the reaction

$$Sr^{2+} + CaCO_3 \rightarrow SrCO_3 + Ca^{2+} \quad (03)$$

we again calculated the enthalpy change ($\Delta H°$) as $\Delta H° = -11.3$ kJ/mol. The van't Hoff equation predicts that the Sr/Ca content of a thermodynamically ideal aragonite will decrease by ~1.7% per degree between 0° and 30°C. Note that both inorganic experiments (Kinsman and Holland, 1969) and calibrations of Sr dependence in reef corals (Gagan, 2000) indicate a significantly weaker dependence on temperature of ~ 0.4–0.9% per degree.

The difference in average temperature between treatment groups equals 5.7°C (17.1–11.4, from Table 1). A 5.7°C decrease in temperature predicts a 9.7% increase in Sr/Ca. Results from this study demonstrate that with the 5.7°C decrease in temperature, Sr/Ca increased ~ 10% for statolith, suggesting the possibility for thermodynamic control on statolith Sr/Ca. However, protoconch Sr/Ca exhibited the opposite Sr-temperature relationship, implying that protoconch Sr/Ca is probably not under thermodynamic control.

Using thermodynamic constants to calculate the temperature dependency of metal incorporation provides a starting point that can be compared to experimentally determined results. However, equilibrium thermodynamic calculations do not take into account kinetic processes that affect trace element incorporation in precipitated calcite and aragonite (Rimstidt et al., 1998). For example, because trace metals are incorporated into aragonite at a different rate than calcium, a solution boundary layer results, with enrichment or depletion of the trace element in the boundary layer dependent upon the rate of transport of ions from the surrounding solution to the crystal surface. This can result in oscillatory zoning within the growing crystal. A second important kinetic process is due to different adsorption sites on the crystal face having differing energies, which results in different tendencies for trace metals to attach at kink sites located along the growing surface of the crystal. This causes sector zoning within the growing crystal. Both of these processes can influence the temperature dependence of trace metal incorporation (Rimstidt et al., 1998) and may help to explain the differences in temperature dependence observed between our results in statoliths and those seen in inorganic experiments and coral. The positive temperature dependence observed for Sr incorporation into protoconch (see Discussion), which is opposite to the thermodynamic prediction, suggests that biologic and/or kinetic processes have the potential to overwhelm the thermodynamic tendency.

APPENDIX 2

Table A1. Ba/Ca (μmol/mol) for protoconch and statolith per treatment per flask from encapsulated lab cultured *Kelletia kelletii* larvae. Statolith values are averages (±1 standard error) of ten laser-ablated statoliths per flask. Asterisks indicate samples lost during cleaning preparation steps.

Flask	Ba/Ca (μmol/mol) seawater	Temp (°C)	Ba/Ca (μmol/mol) protoconch	Average Ba/Ca (μmol/mol) statolith ±1 SE
1	3.47	11.4	4.36	6.46 ± 0.21
2	3.47	11.4	4.32	7.99 ± 0.39
3	3.47	11.4	3.70	6.91 ± 0.22
4	3.47	17.1	3.94	4.34 ± 0.10
5	3.47	17.1	4.23	5.61 ± 0.17
6	3.47	17.1	4.05	4.79 ± 0.12
7	6.31	11.4	7.61	8.51 ± 0.31
8	6.31	11.4	6.74	8.78 ± 0.55
9	6.31	11.4	7.06	13.74 ± 0.53
10	6.31	17.1	—*	7.59 ± 0.13
11	6.31	17.1	6.01	8.27 ± 0.27
12	6.31	17.1	5.54	7.75 ± 0.24
13	11.78	11.4	12.68	16.08 ± 0.58
14	11.78	11.4	13.28	18.41 ± 0.38
15	11.78	11.4	13.88	23.56 ± 1.06
16	11.78	17.1	11.08	14.03 ± 0.33
17	11.78	17.1	11.67	16.84 ± 0.67
18	11.78	17.1	10.18	16.52 ± 0.83
19	17.49	11.4	16.46	26.28 ± 0.76
20	17.49	11.4	22.78	26.65 ± 0.54
21	17.49	11.4	19.62	27.28 ± 1.31
22	17.49	17.1	14.93	20.69 ± 0.58
23	17.49	17.1	—*	25.76 ± 0.83
24	17.49	17.1	13.77	19.87 ± 0.72

Table A2. ANOVA table and test statistics on log transformed larval protoconch Ba/Ca ratios testing the hypotheses of no effect of seawater (SW) Ba/Ca, no effect of temperature (T), and no interaction effect between seawater Ba/Ca and temperature on Ba incorporation into protoconch aragonite.

Source	SS	DF	MS	F ratio	Prob > F
Ba/Ca SW	5.89	3	1.96	235.83	<0.0001
T	0.15	1	0.15	18.38	0.0011
T × Ba/Ca SW	0.06	3	0.02	2.29	0.1303
Error	0.10	12	0.01		
Total	6.10	19			

Table A3. Nested ANOVA table and test statistics for log transformed larval statolith Ba/Ca ratios testing the hypotheses of no effect of seawater (SW) Ba/Ca, no effect of temperature (T), and no interaction effect between seawater Ba/Ca and temperature on Ba incorporation into statolith aragonite. Statoliths were nested within cultures (C), within seawater Ba/Ca, and within temperature.

Source	SS	DF	MS	F ratio	Prob > F
Ba/Ca SW	72.99	3	24.33	115.69	<0.0001
T	3.74	1	3.74	17.80	0.0007
T × Ba/Ca SW	0.30	3	0.10	0.48	0.7031
C (Ba/Ca SW, T)	3.37	16	0.21	16.03	<0.0001
Stato (C,Ba/CaSW,T)	2.82	215	0.01		
Total	83.17	238			

Table A4. ANOVA table and test statistics on larval protoconch Sr/Ca ratios testing the hypothesis of no effect of temperature (T) on Sr incorporation into protoconch aragonite.

Source	SS	DF	MS	F ratio	Prob > F
Model	0.60	1	0.60	18.42	0.0004
Error	0.59	18	0.03		
Total	1.19	19			

Table A5. Nested ANOVA table and test statistics for log transformed larval statolith Sr/Ca ratios testing the hypothesis of no effect of temperature (T) on Sr incorporation into statolith aragonite. Statoliths were nested within cultures (C) and within temperature.

Source	SS	DF	MS	F ratio	Prob > F
T	0.69	1	0.69	74.08	0.001
C (T)	0.04	4	0.01	1.51	0.213
Stato (C, T)	0.33	54	0.01	0.62	0.981
Total	2.86	238			